J Assist Reprod Genet (2010) 27:299–307
DOI 10.1007/s10815-010-9409-4

GAMETE BIOLOGY

The expression pattern of SEPT7 correlates with sperm morphology

Hsin-Chih Albert Chao · Ying-Hung Lin · Yung-Che Kuo · Chiung-Jiung Shen · Hsian-Ann Pan · Pao-Lin Kuo

Received: 14 November 2009 / Accepted: 11 March 2010 / Published online: 30 March 2010

Abstract
Purpose To investigate the expression pattern of the SEPT7 protein during spermatogenesis and its potential role in sperm function.
Methods We first investigated the expression pattern of SEPT7 during different steps of mouse spermiogenesis using an immunofluorescence assay (IFA). IFA was also applied to study the expression pattern of SEPT7 in human ejaculated spermatozoa. Nine fertile men with normal semen parameters were used as the control group, and 21 infertile men with asthenozoospermia were recruited as the patient group. We assessed the frequency of the SEPT7 signal in the various morphological subgroups.
Results In humans, the frequency of a defective SEPT7 signal was significantly increased in men with asthenozoospermia. The absence of a SEPT7 signal was more prevalent in sperm containing morphological defects of various types.
Conclusions The expression pattern of SEPT7 suggested that this protein may be involved in the regulation of subcellular-compartment formation during spermiogenesis in the mouse. The absence of a SEPT7 signal correlated with multiple sperm defects.

Keywords Compartmentalization · Expression pattern · SEPT7 · Spermiogenesis · Sperm morphology

Hsin-Chih Albert Chao and Ying-Hung Lin contributed equally to this work

Capsule The expression pattern of SEPT7 in spermatozoa suggests its importance for subcellular-compartment formation during spermiogenesis. Absence of SEPT7 signal correlated with asthenozoospermia and abnormal sperm morphology.

H.-C. A. Chao
Division of Obstetrics and Gynecology, National Cheng Kung University College of Medicine and Hospital, Dou-Liou Branch, Yunlin, Taiwan
e-mail: chao531018@hotmail.com

Y.-H. Lin · Y.-C. Kuo
Graduate Institute of Basic Medical Sciences College of Medicine, National Cheng Kung University, Tainan, Taiwan

C.-J. Shen
Department of Biological Science and Technology, Chung Hwa College of Medical Technology, Tainan, Taiwan

H.-A. Pan · P.-L. Kuo (✉)
Department of Obstetrics and Gynecology, College of Medicine, National Cheng Kung University, Tainan, Taiwan
e-mail: paolink@mail.ncku.edu.tw

Introduction

Septins belong to a family of evolutionarily highly conserved cytoskeletal proteins with GTPase activity. In humans, a total of 14 members have been identified in this superfamily, and all family members exhibit various alternative splicing isoforms [1]. Septins are involved in many biological functions, which include scaffolding for different mitosis-related molecules, vesicle trafficking, and exocytosis, and they act as a diffusion barrier for proper compartmentalization. Some isoforms are implicated in mitochondrial function and apoptosis [2–4]. A comprehensive microarray study showed that most septins are expressed ubiquitously (SEPT2, SEPT4, SEPT6, SEPT7, SEPT8, SEPT9, SEPT10, and SEPT11) and that several of these proteins (SEPT3, SEPT4, SEPT5, SEPT7, SEPT8, and SEPT11) exhibit enhanced expression in specific tissues, such as the central

nervous system (CNS). It is of note that some septin splice variants also appear to be expressed in a tissue-specific manner [5].

There is increasing evidence of the involvement of septins in the pathogenesis of various human diseases, including neoplasia, neurodegenerative conditions, infection, and infertility [1, 6–8]. Among the 14 septin family members, SEPT4 and SEPT12 play important roles in the differentiation of postmeiotic germ cells. SEPT4 is expressed at the annulus, which is a ring-like structure located between the midpiece and the tail region of spermatozoa. During spermatogenesis, SEPT4 is essential for the maintenance of proper mitochondrial architecture and for the establishment of the annulus. *Septin4* null mice are viable; however, males are sterile because they produce immotile sperm with a defective annulus [7, 8]. In humans, disorganized annulus/SEPTIN rings were identified in a subset of patients with asthenozoospermia [9, 10]. SEPT12 is also a component of the sperm annulus [6]. To explore the role of SEPT12 in mammalian spermatogenesis, we knocked out the *Septin12* gene in mouse ES cells via gene targeting. Chimeric mice exhibit severe spermatogenic defects, and their reproductive phenotypes include low testis weights, abnormal testicular histology (hypospermatogenesis or mature arrest of male germ cells), and increased apoptosis of germ cells, immotile sperm, sperm with a bent or broken tail, and sperm with acrosomal and mitochondrial defects. We also found a significant loss of SEPT12 in sperm samples from men with asthenozoospermia. Our results indicate that SEPT12 plays critical roles during terminal differentiation of male germ cells in both mice and humans [11].

The *SEPTIN7* gene is located on human chromosome 7p14.3, and alternative splicing of the gene results in the transcription of two isoforms. SEPT7 is critical for spine morphogenesis and dendrite development in neurons [12]. SEPT7 is also one of the structural constituents of the annulus of human and mouse sperm [8]. A terato-asthenozoospermic patient exhibited the absence of an annulus in 97% of his ejaculated spermatozoa, in which normal SEPT4/7 signals at the annulus were also lacking. Although both proteins are expressed, they are not properly localized in these sperm cells [9]. Another study revealed the presence of a defective annulus/SEPT4/7 phenotype in some patients with asthenozoospermia. Thus, SEPT4/7 may be used as a biomarker for monitoring the status of spermiogenesis [10]. To explore the role of SEPT7 in spermiogenesis, we investigated the expression pattern of SEPT7 during different steps of mouse spermiogenesis. We also analyzed the SEPT7 signal in human semen samples. We found that the absence of a SEPT7 signal was more prevalent in immature sperm and in sperm with head, neck, and tail defects. Our findings suggest strongly that SEPT7 is involved in the regulation of sperm maturation.

Materials and methods

Patients and semen samples

This study was approved by the Institutional Review Board of the National Cheng Kung University Hospital. We recruited 21 infertile men presenting with asthenozoospermia including nineteen moderate asthenozoospermic patients (the percentage of motile sperm ranging from 17% to 46%) and two patients with severe asthenozoospermia (the percentage of motile sperm being 0% and 14%, respectively). The percentages of sperm with various morphological categories were similar between the moderate and severe patients. The infertile men underwent semen analysis because they all had difficulty in conceiving a child. Nine fertile men with normal semen parameters were collected as the control group. The semen characteristics in the two groups were as follows, respectively: sperm count, 72.63±50.8 and 119.0±33.1×10^6 spermatozoa / ml; motility, 31.2±12.4% and 69.8±11.9% (mean ± standard deviation (SD)) (Table 1). For semen analysis, ejaculates were obtained by masturbation after a minimum of 48 h of sexual abstinence. Semen analysis was performed according to the protocol recommended by the World Health Organization

Table 1 Semen characteristics of control subjects and patients

	Fertile control (n=9)	Asthenozoospermic men (n=21)	p-value
Semen characteristics			
Concentration (×10^6 spermatozoa/mL)	119.0±33.1	72.6±50.8	**0.0184**
Motility (%)	69.8±11.9	31.2±12.4	**<0.0001**
Percentage of morphological defects and immaturity (%)			
Head defects	17.2±11.3	15.9±8.61	0.8034
Neck defects	4.20±2.07	5.10±3.75	1.0000
Tail defects	5.80±3.74	18.9±13.3	**0.0248**
Immature	8.11±3.26	9.26±8.67	0.4284

All values are showed as mean ± SD, the bold number indicate statistical significance

using a modified Neubauer chamber (WHO, 1999). Two laboratory technicians performed the analyses of the ejaculates. The interobserver coefficient of variation was low (9.3%) regarding concentration assessment. The diagnoses of asthenozoospermia and oligoasthenozoospermia were based on at least two separate semen analyses and two separate centrifuged semen sample analyses (3,000× *g* for 15 min). All patients received detailed clinical evaluation, which included assessment of hormonal profiles (luteinizing hormone (LH), follicle stimulating hormone (FSH), prolactin, and testosterone) and physical examination.

Immunofluorescence assay (IFA) of mouse testicular tissues

Testicular tissues were collected from adult male mice using methods described in a previous study [13]. For immuno-fluorescence staining, the slides were treated with 0.1% Triton X-100, washed twice with Tris-buffered-saline (TBS), followed by incubation with the anti-SEPT7 antibody (1:200) for 60 min at room temperature. Following the washing steps with TBS, sections were exposed to goat - anti-rabbit Alexa Flour 488 (Molecular Probes, Carlsbad, CA, USA) for 60 min at room temperature and washed with TBS. Lectin peanut agglutinin (PNA)-conjugated with Alexa Fluor 568 (10 mg/ml) (Molecular Probes, Carlsbad, CA, USA) was used to locate the acrosomes in testes and spermatozoa. The midpiece of spermatozoa was staining by the mitochondrial tracker (Molecular Probes, Carlsbad, CA, USA). DAPI was used to stain the nuclei. Labeled spermatozoa were examined and images were captured using the upright microscopy system BX60 (Olympus, Tokyo, Japan).

Preparation of murine testicular spermatogenic cells and spermatozoa

Mouse spermatogenic cells were collected as described previously [15]. In brief, testes were excised, decapsulated, and cut into small pieces. After enzyme digestion, germ-cell suspensions were filtered through 35 μM nylon filters (Falcon; Becton Dickinson, Franklin Lakes, NJ, USA), followed by centrifugation using a Kubota centrifuge 3330 (Kubota Corp., Tokyo, Japan). Germ cells at different developmental stages were collected. Mature spermatozoa were collected from the cauda epididymis of adult male mice.

IFA of mouse spermatozoa

IFA was performed to investigate the expression pattern of mouse spermatogenic cells and spermatozoa, according to the protocol described in our previous paper [14]. Briefly, spermatogenic cells and spermatozoa were spread on a slide and air dried. The slides were treated with 0.1% Triton X-100, washed twice with TBS, followed by incubation with the anti-SEPT7 antibody (1:200 dilution) for 60 min at room temperature. Tissue sections were then exposed to the swine anti-rabbit IgG conjugated with FITC for 60 min at room temperature and washed with TBS. The slides were subsequently counterstained with MitoTracker. The nuclei of the isolated proximal tubules were labeled with DAPI and were then dissolved in PBS (pH7.4) for 5 min, washed with 1× PBS, and mounted. An additional slide stained only with anti-rabbit IgG was used as a control. Labeled spermatozoa were examined and images were captured using the upright microscopy system BX60.

Assessment of sperm morphology and IFA in human samples

Human semen samples were collected from nine fertile men with normal semen parameters and 21 infertile men with asthenozoospermia. Semen samples were ejaculated into sterile containers, liquefied at 37°C for 30 min, spread on a slide, air dried, and stocked at −80°C until use. For each subject, an average of 100 sperm cells was evaluated for sperm morphology and SEPT7 signal. Individual sperm cells were categorized as having normal or abnormal morphology (including head, neck, and tail defects and immaturity) according to the WHO criteria (WHO, 1999). The IFA experimental procedures and image analysis were described in the previous section.

Statistical analyses

Spermatozoa were grouped according to morphological abnormalities. An unpaired *t* test was used to compare the differences in the percentage of the SEPT7 signal among the different types of morphological abnormalities. A P value$<$ 0.05 was considered significant. We used the Prism statistical package version 4.0 (GraphPad, San Diego, CA, USA) for statistical analyses.

Results

Expression pattern of SEPT7 in mouse germ cells

In mouse testis sections, SEPT7 was expressed in the spermatocyte, round spermatid and elongated spermatid in the lumen of seminiferous tubules (Fig. 1). Given that the expression of SEPT7 in postmeiotic germ cells, we applied IFA to the study its expression pattern in different steps of spermiogenesis using fractionated germ cells. Early in spermiogenesis (step 9), SEPT7 was diffusely dispersed in the cytoplasm of round spermatid. The protein was aggregated at the perinuclear area as a circular structure

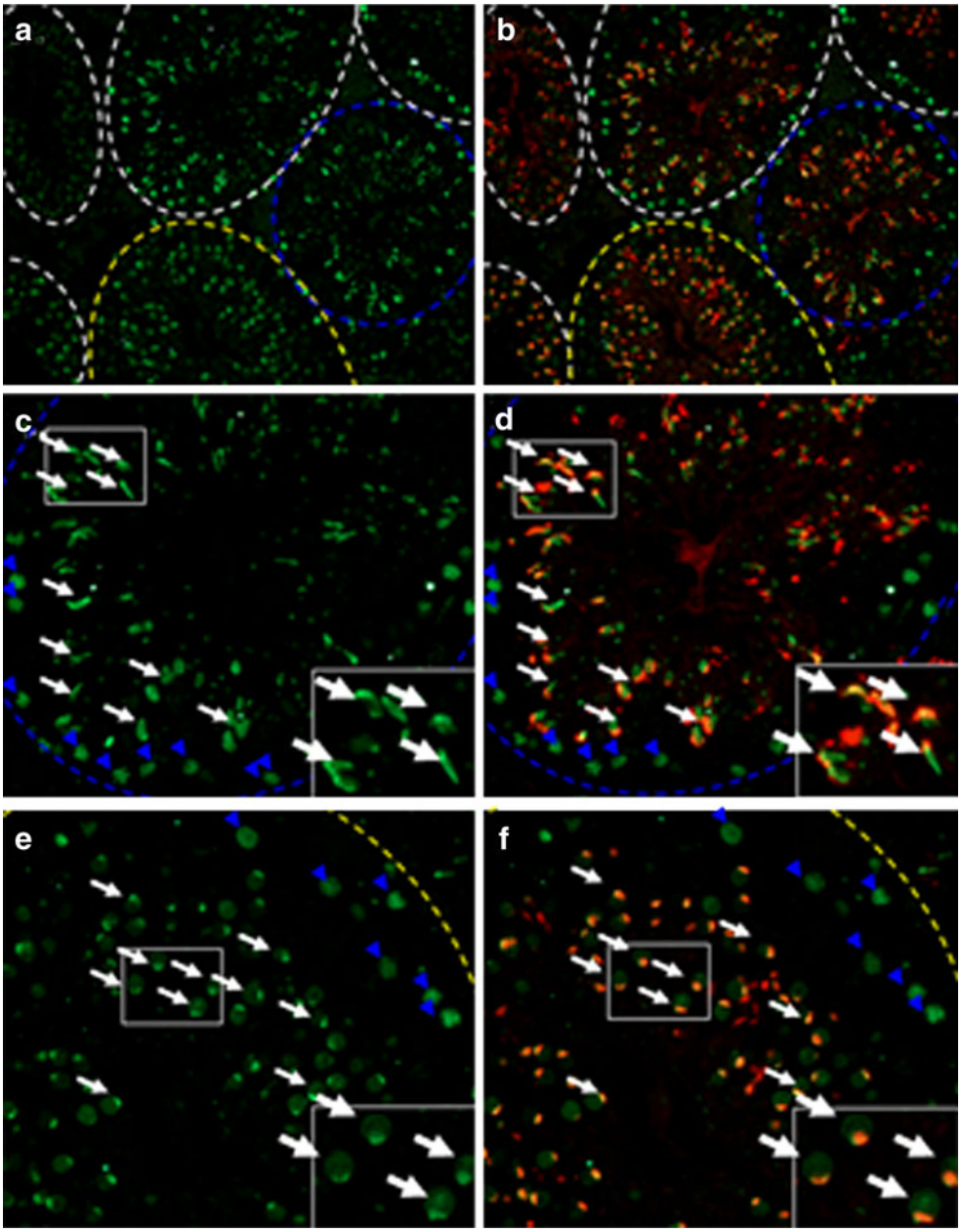

Fig. 1 Immunofluorescence assay of SEPT7 in the seminiferous tubule of the mouse testis. SEPT7 (green) was expressed at the spermatocyte (*blue arrowhead*) and spermatid (*white arrow*). **a** and **b**: general view of the mouse testis; **c** and **d** (stage IX-X of spermatogenesis); **e** and **f** (Stage IV–V of spermatogenesis). The inlets show enlarged pictures. The stage of spermatogenesis was judged according to the acrosome morphology. Green (SEPT7); Red (Lectin for acrosome)

(which is termed the perinuclear ring of the manchette) and was also concentrated at the caudal region of the cytoplasm, where it colocalized with mitochondria (Fig. 2a). At around step 10–11, the mitochondrial and SEPT7 signals were displaced toward the caudal part of the sperm. With the development of the sperm tail, SEPT7 signals became more condensed at the elongated caudal part of the cell, together with mitochondria. SEPT7 signals were also concentrated at the circular structure between the acrosome and the nucleus (Fig. 2b). In a more advanced step of spermiogenesis (step 14), SEPT7 was detected as two dots at the neck and at the annulus region, with disappearance of the perinuclear ring (Fig. 2c, i–l). At step 16, SEPT7 was well distributed in the cytoplasm. At this stage, the protein also colocalized with mitochondria and the nucleus. In mature spermatozoa (Fig. 2d, m–p) obtained from the cauda region of the epididymis, SEPT7 was expressed mainly in the head and in the annulus and faintly in the midpiece. Co-staining for SEPT7 and acrosome showed the similar findings: SEPT7 migrated from the cytoplasm (where it was more concentrated in the perinuclear region) in the round and elongating spermatid to the annulus in the elongated spermatid and mature spermatozoa (Fig. 3).

Expression pattern of SEPT7 in human mature spermatozoa

Table 1 shows that the sperm concentration was significantly lower in the asthenozoospermia group compared

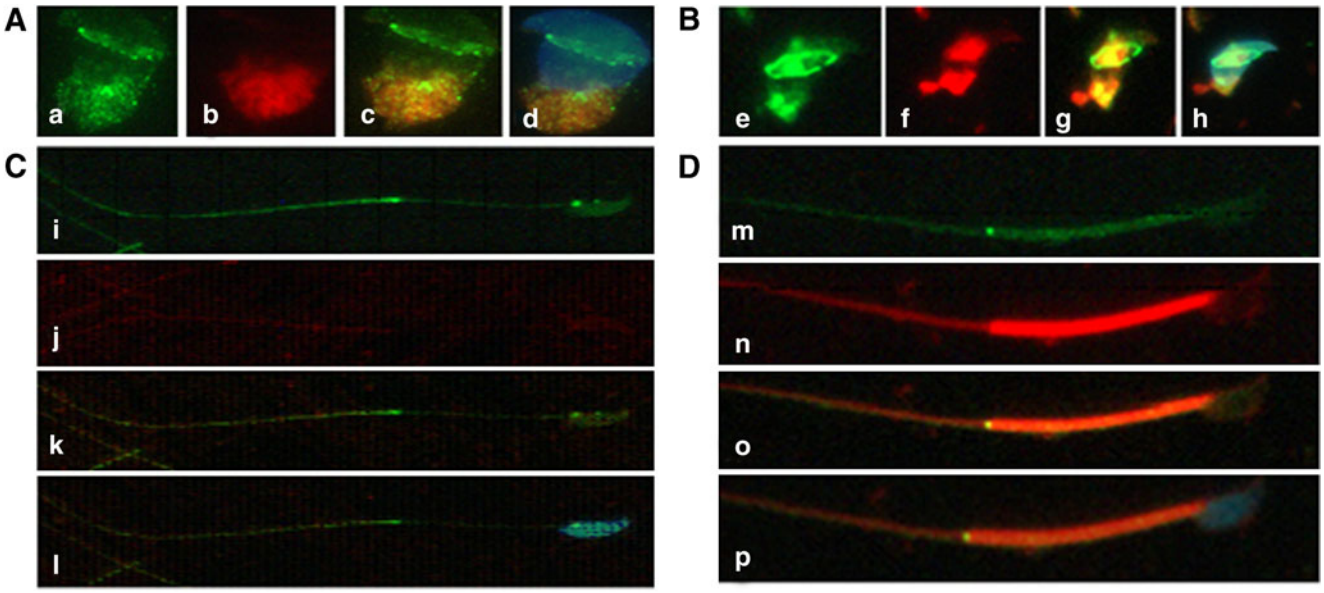

Fig. 2 Immunofluorescence assay of SEPT7 (green) and mitochondria (MitoTracker, red) in developing spermatozoa (**I–IV**). **I** and **II** (a–h) indicate early spermiogenesis. In the round spermatid (**I**, a–d), mitochondria are localized at the opposite side of the nucleus. With advancing spermiogenesis (**II**, e–h), the tail starts to develop and the mitochondria are divided into two parts. With the elongation of the tail (**III**, i–l), the mitochondria are diffused into the tail region. At this stage, SEPT7 was localized predominantly at the neck and the annulus. In mature sperm (**IV**, m–p), SEPT7 appeared mainly as a bright dot signal at the annulus. It also exhibited a punctate pattern at the mitochondrial sheath and at the head. The nucleus was stained with DAPI (blue)

with the normal group (P=0.0184). The percentage of various morphological defects and immaturity was not significantly different between these two groups, with the exception of the percentage of tail defects, which was significantly higher in the asthenozoospermic group than it was in the normal group (P=0.0248). In mature spermatozoa obtained from ejaculate semen, SEPT7 was most intensely expressed in the annulus, where it colocalized with SEPT4. SEPT7 was also expressed in the sperm head, at highest concentration in the caudal pole (Fig. 4).

The loss of SEPT7 signal was more prevalent in sperm with various types of abnormal morphologies, including immature sperm. We analyzed the frequency of the SEPT7 signal in ejaculated spermatozoa from control subjects and asthenozoospermic patients. Five morphological subgroups were identified according to the WHO (1999) criteria; these included normal, head-defective, neck-defective, tail-defective, and immature cells. Figure 5 depicts several representative examples of sperm morphological defects. In general, the absence of a SEPT7 signal was increased in semen samples with asthenozoospermia (n=21) compared with semen samples from fertile men with normal semen parameters (n=9; P<0.0001, unpaired t test; Fig. 6a). In fertile men with normal semen parameters, the percentage of defective signals was significantly increased in head-defective and immature sperm (P=0.0489 and 0.0098, respectively; Fig. 6b). In asthenozoospermic patients, the percentage of absent SEPT7 signal was significantly higher in all four morphologically defective groups (P<0.0001, <0.0001, <0.0001, and =0.002 for head-defective, neck-defective, tail-defective, and immature sperm cells, respectively; Fig. 6c). The combination of results from both groups revealed that a normal SEPT7 signal was significantly decreased in all four groups of sperm with abnormal morphology (P<0.0001, =0.002, <0.0001, and <0.0001 for head-defective, neck-defective, tail-defective, and immature sperm cells, respectively; Fig. 6d). Although the sample

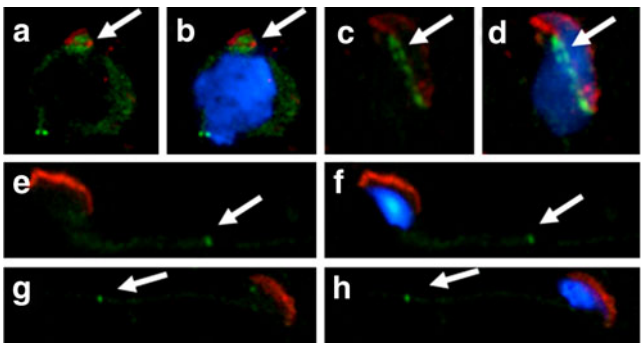

Fig. 3 Immunofluorescence assay of SEPT7 (green) and acrosome (Lectin, red) in developing spermatozoa. **a, b**: Round spermatids; **c, d**: Elongating spermatids; **e, f**: Elongated spermatids; **g, h**: mature spermatozoa. SEPT7 migrates from the cytoplasm (concentrated in the perinuclear region) to the annulus during sperm maturation. **a**, **c**, **e** and **g**: merged pictures for SEPT7 and Lectin; **b**, **d**, **f** and **h**: merged pictures for SEPT7, Lectin and DAPI. The nucleus was stained with DAPI (blue)

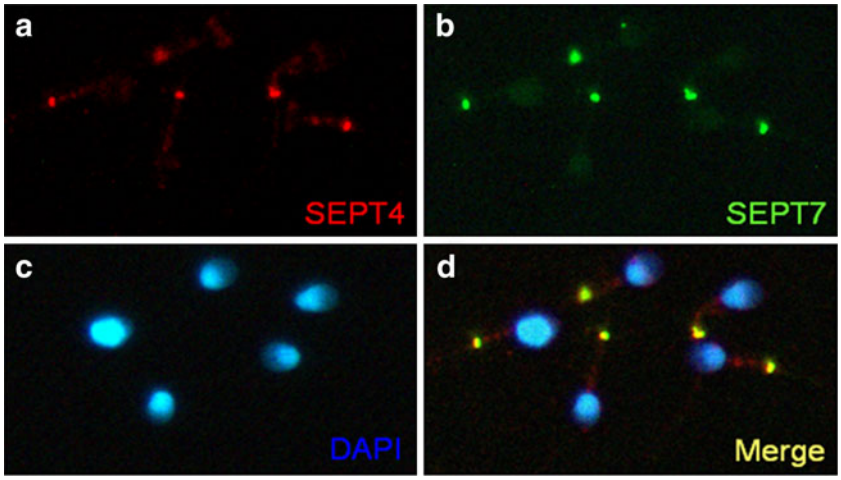

Fig. 4 Expression patterns of SEPT7 and SEPT4 in human sperm. **a**, Immunofluorescence assay (IFA) showed that SEPT4 (red) was localized predominantly at the annulus region. **b**, Strong SEPT7 (green) signal at the annulus and faint signal at the head. **d**, SEPT4 and SEPT7 overlapped completely at the annulus. **c**, The nucleus was stained with DAPI (blue)

size is too small to draw a meaningful conclusion, the degree of asthenozoospermia seems to correlate with percentage of defective SEPT7 signals. The percentage of sperm with defective SEPT7 signals was 19.1% and 36.1%, respectively, in sperm with normal morphology. The percentage increased to 50.7% and 90.3%, respectively, in the abnormal sperm for these two patients.

Discussion

The perinuclear ring and the inserted microtubular mantle wrapping the spermatid nucleus create the manchettes during the round-to-elongating transition [16–18]. Because of its spatial localization and tight association with the spermatid nucleus, the manchette/perinuclear ring plays a principal role in the molding of the spermatid nucleus. CLIP-170 is a microtubule plus-end-tracking protein that is associated with the spermatid manchette. Male mice carrying homozygous knockout of *CLIP-170* are subfertile and produce sperm with abnormal heads [19]. Our finding suggests that SEPT7 may contribute to the formation of the perinuclear ring of the manchette. δ-tubulin has been proposed as a central component of the perinuclear ring [20]. SEPT7 expression emerged at step 9 and disappeared at step16 of spermiogenesis, which is an expression pattern that is similar to that of δ-tubulin. SEPT7 may interact with δ-tubulin in the assembly or positioning of the perinuclear

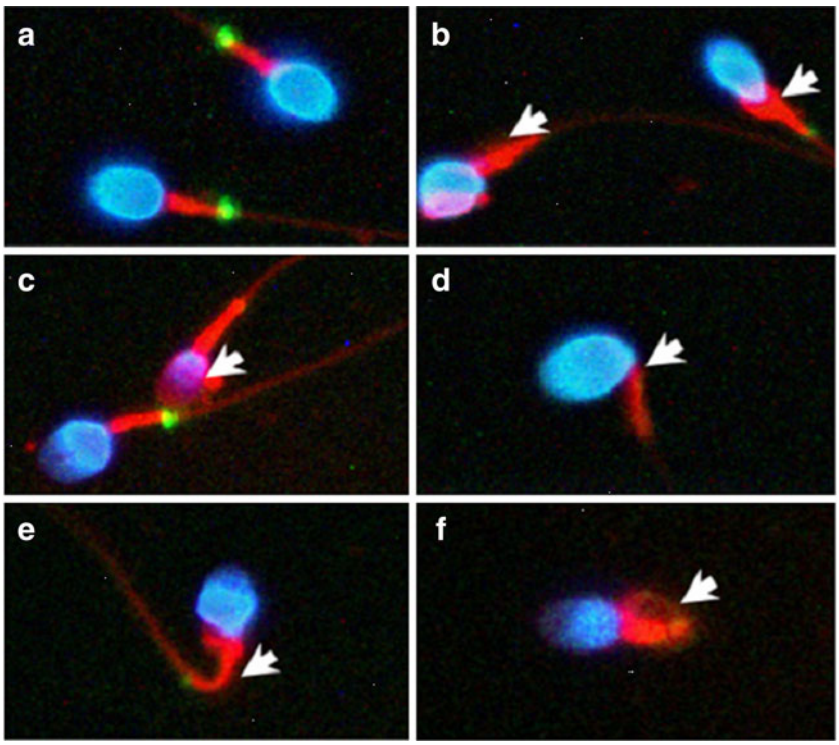

Fig. 5 Human spermatozoa with various types of morphological defects. **a**, Normal spermatozoa. **b**, An immature sperm with a cytoplasmic droplet. **c**, A head-defective sperm with loss of nuclear content. **d**, A neck-defective sperm with a bent neck. **e** and **f**, Tail-defective sperm with bent (**e**) or coiled (**f**) tails. The defects are indicated by the white arrows. Blue, nuclei stained with DAPI; red, mitochondria stained with MitoTracker; green, SEPT7

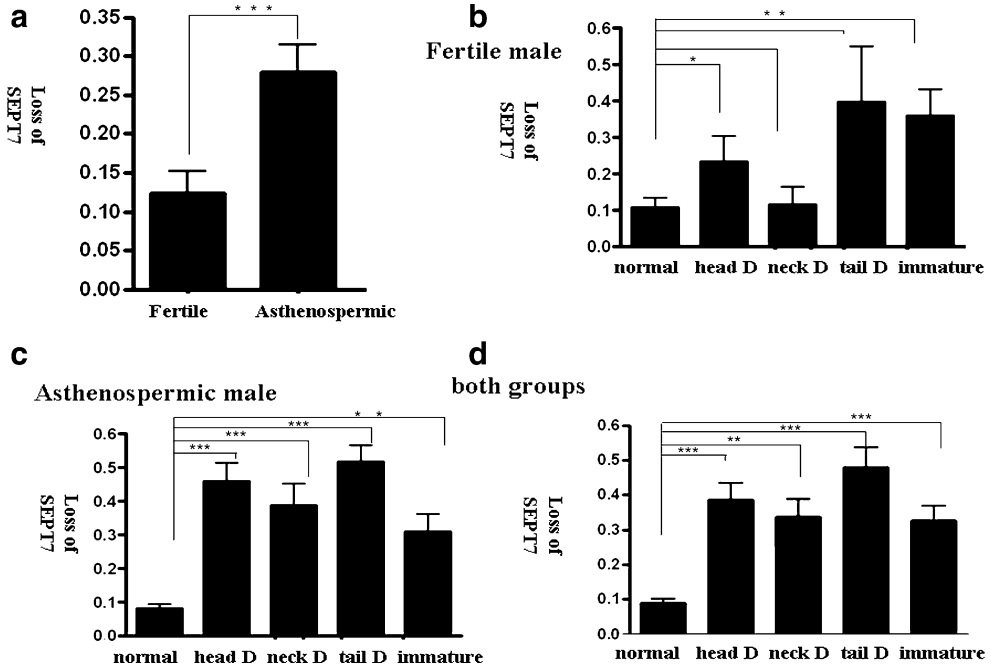

Fig. 6 Loss of SEPT7 signal was associated with motility and morphological defects of spermatozoa. The Y-axis indicates the frequency of absent SEPT7 signal in spermatozoa (defined as the number of spermatozoa without SEPT7 signal/the total number of spermatozoa scored). The spermatozoa were divided into five subgroups according to morphological criteria: normal sperm (normal), sperm with head defects (head D), sperm with neck defects (neck D), sperm with tail defects (tail D), and immature sperm (immature). **a**, The percentage of sperm with loss of SEPT7 signal was increased in semen samples of asthenozoospermic men (asthenozoospermic) compared with men with normal semen parameters (fertile; $P<0.0001$, unpaired t test). **b**, In fertile men, the percentage of sperm with an absence of SEPT7 signal was significantly higher in head-defective and immature sperm. In asthenozoospermic men (**c**) and in a combined analysis of the two groups (**d**), the percentage of sperm with an absence of SEPT7 signal was significantly higher in all groups with morphological defects. $*P<0.05$; $**P<0.01$; $***P<0.001$; unpaired t test. Error bars indicate ± SD

ring during spermiogenesis, considering the prevailing evidence of an interaction between septins and tubulins in mammals [1, 21, 22]. It is also attractive to speculate that SEPT7 dysfunction may interfere with manchette/perinuclear ring formation and with resultant sperm-head defects.

In this study, we also found that SEPT7 migrated from the midpiece to the annulus as spermatozoa matured. This expression pattern suggests that SEPT7 may be involved in the regulation of the formation of the midpiece and annulus. Previous studies showed that SEPT1/4/6/7/12 are located at the sperm annulus and that this septin-based organization is a requisite for the structural and functional integrity of sperm [7, 8, 11, 23]. Other proteins located at the mouse sperm annulus include DNAJB13 [24] and testis anion transporter 1 (TAT1) [25]. In the mouse, gene targeting of *Septin4*, *Septin12*, and *Tat1* lead to abnormal mitochondrial organization and tail defects [6, 7, 11, 25]. In humans, absence of the annulus is associated with abnormal mitochondrial organization in poor-motility sperm [9]. A recent study showed that DNAJB13, which is a type II HSP40, attaches itself to the annular anlage and then recruits septins via direct interaction with SEPT4 or a SEPT4-containing septin complex for the formation of an authentic annulus in the early stage of sperm flagellum morphogenesis. In the late stage, it may assist the migration of the annulus and direct the annulus to the junction where SEPT4/7 are localized [24]. It is likely that SEPT7 may act directly or indirectly with DNAJB13 to orchestrate the formation of the sperm midpiece and tail. Considering that the abnormal localization of the annulus may result in the absence of a mitochondrial sheath [26], it is attractive to speculate that SEPT7 dysfunction may result in the failure of the midpiece to reach its normal position along the flagella, which results in sperm with neck and tail defects.

This study constitutes the first description of the expression pattern of SEPT7 during spermiogenesis. The expression pattern of SEPT7 was reminiscent of that observed for SEPT12 in the post-meiotic germ cell [11]. The expression pattern suggested that SEPT7/SEPT12 may regulate the formation of all four subcellular compartments (i.e., acrosome, head, midpiece, and tail) jointly during spermiogenesis. It is possible that SEPT7 filaments serve as intracellular diffusion barriers (e.g., the perinuclear ring and the annulus) between the different subcellular compartments of sperm.

We also demonstrated for the first time the correlation between sperm immaturity and loss of SEPT7 signal in human spermatozoa. Sperm maturation involves removal of surplus cytoplasm, cytoplasmic membrane remodeling, chromatin condensation, tail sprouting, and acrosome formation [27]. The immature sperm is associated with poor sperm motility, lower fertilizing capacity, reduced binding to the zona pellucida, increased rate of aneuploidies, and nuclear DNA damage [28]. Among the various morphological markers of immature sperm, the retention of cytoplasm in the midpiece and a shorter tail length are the most prominent characteristics of immature sperm [29]. Two biochemical markers have also been proposed as representative of sperm maturity: creatine kinase (CK) activity [30] and CK-M isoform ratio [31, 32]. Our findings may add SEPT7 to the list of sperm-maturity markers. The surplus cytoplasm is completely removed around the time of ejaculation via an unidentified mechanism [33]. Considering that *Septin4* knockout mice also exhibit increased rates of immature sperm [7, 8], SEPT4/7 may participate jointly in the regulation of the removal of the residual cytoplasm during sperm maturation.

Septins form homo- and heterooligomeric complexes that are assembled into filamentous structures depending on the combination of the various septin members in mammals [1, 34]. Considering the high similarity of the expression patterns of SEPT4, SEPT7, and SEPT12, it is highly likely that the SEPT4/7/12 complex not only constitutes the structural basis of the annulus but also serves as a diffusion barrier between the various subcellular compartments of mammalian spermatozoa [6, 11, 35, 36]. As alterations in the expression of one septin can lead to altered expression of other septins [5], the concomitant use of multiple markers (SEPT4 + SEPT7 + SEPT12) may be superior to any single marker as a sperm-quality index.

Conclusions

SEPT7 may be involved in the regulation of subcellular-compartment formation, as it correlated with the morphology and maturity of sperm.

Acknowledgments This study was supported by grants from the National Science Council of the Republic of China (NSC95-2314-B-006-011, NSC96-2314-B-006-003, and NSC97-2622-B-006-002-CC1).

References

1. Hall PA, Russell SE. The pathobiology of the septin gene family. J Pathol. 2004;204:489–505.
2. Elhasid R, Sahar D, Merling A, Zivony Y, Rotem A, Ben-Arush M, et al. Mitochondrial pro-apoptotic ARTS protein is lost in the majority of acute lymphoblastic leukemia patients. Oncogene. 2004;23:5468–75.
3. Takahashi S, Inatome R, Yamamura H, Yanagi S. Isolation and expression of a novel mitochondrial septin that interacts with CRMP/CRAM in the developing neurones. Genes Cells. 2003;8:81–93.
4. Larisch S, Yi Y, Lotan R, Kerner H, Eimerl S, Parks WT, et al. A novel mitochondrial septin-like protein, ARTS, mediates apoptosis dependent on its P-loop motif. Nat Cell Biol. 2000;2:915–21.
5. Hall PA, Jung K, Hillan KJ, Russell SE. Expression profiling the human septin gene family. J Pathol. 2005;206:269–78.
6. Steels JD, Estey MP, Froese CD, Reynaud D, Pace-Asciak C, Trimble WS. Sept12 is a component of the mammalian sperm tail annulus. Cell Motil Cytoskeleton. 2007;64:794–807.
7. Kissel H, Georgescu MM, Larisch S, Manova K, Hunnicutt GR, Steller H. The Sept4 septin locus is required for sperm terminal differentiation in mice. Dev Cell. 2005;8:353–64.
8. Ihara M, Kinoshita A, Yamada S, Tanaka H, Tanigaki A, Kitano A, et al. Cortical organization by the septin cytoskeleton is essential for structural and mechanical integrity of mammalian spermatozoa. Dev Cell. 2005;8:343–52.
9. Lhuillier P, Rode B, Escalier D, Lores P, Dirami T, Bienvenu T, et al. Absence of annulus in human asthenozoospermia: case report. Hum Reprod. 2009;24:1296–303.
10. Sugino Y, Ichioka K, Soda T, Ihara M, Kinoshita M, Ogawa O, et al. Septins as diagnostic markers for a subset of human asthenozoospermia. J Urol. 2008;180:2706–9.
11. Lin YH, Lin YM, Wang YY, Yu IS, Lin YW, Wang YH, et al. The expression level of septin12 is critical for spermiogenesis. Am J Pathol. 2009;174:1857–68.
12. Tada T, Simonetta A, Batterton M, Kinoshita M, Edbauer D, Sheng M. Role of septin cytoskeleton in spine morphogenesis and dendrite development in neurons. Curr Biol. 2007;17:1752–8.
13. Rawe VY, Ramalho-Santos J, Payne C, Chemes HE, Schatten G. WAVE1, an A-kinase anchoring protein, during mammalian spermatogenesis. Hum Reprod. 2004;19:2594–604.
14. Lin YH, Lin YM, Teng YN, Hsieh TY, Lin YS, Kuo PL. Identification of ten novel genes involved in human spermatogenesis by microarray analysis of testicular tissue. Fertil Steril. 2006;86:1650–8.
15. Yeh YC, Yang VC, Huang SC, Lo NW. Stage-dependent expression of extra-embryonic tissue-spermatogenesis-homeobox gene 1 (ESX1) protein, a candidate marker for X chromosome-bearing sperm. Reprod Fertil Dev. 2005;17:447–55.
16. Greenbaum MP, Ma L, Matzuk MM. Conversion of midbodies into germ cell intercellular bridges. Dev Biol. 2007;305:389–96.
17. Fawcett DW, Anderson WA, Phillips DM. Morphogenetic factors influencing the shape of the sperm head. Dev Biol. 1971;26:220–51.
18. Russell LD, Russell JA, MacGregor GR, Meistrich ML. Linkage of manchette microtubules to the nuclear envelope and observations of the role of the manchette in nuclear shaping during spermiogenesis in rodents. Am J Anat. 1991;192:97–120.
19. Akhmanova A, Mausset-Bonnefont AL, van Cappellen W, Keijzer N, Hoogenraad CC, Stepanova T, et al. The microtubule plus-end-tracking protein CLIP-170 associates with the spermatid manchette and is essential for spermatogenesis. Genes Dev. 2005;19:2501–15.
20. Kato A, Nagata Y, Todokoro K. Delta-tubulin is a component of intercellular bridges and both the early and mature perinuclear rings during spermatogenesis. Dev Biol. 2004;269:196–205.
21. Nagata K, Kawajiri A, Matsui S, Takagishi M, Shiromizu T, Saitoh N, et al. Filament formation of MSF-A, a mammalian septin, in human mammary epithelial cells depends on interactions with microtubules. J Biol Chem. 2003;278:18538–43.
22. Surka MC, Tsang CW, Trimble WS. The mammalian septin MSF localizes with microtubules and is required for completion of cytokinesis. Mol Biol Cell. 2002;13:3532–45.

23. Caudron F, Barral Y. Septins and the lateral compartmentalization of eukaryotic membranes. Dev Cell. 2009;16:493–506.
24. Guan J, Kinoshita M, Yuan L. Spatiotemporal association of DNAJB13 with the annulus during mouse sperm flagellum development. BMC Dev Biol. 2009;9:23.
25. Toure A, Lhuillier P, Gossen JA, Kuil CW, Lhote D, Jegou B, et al. The testis anion transporter 1 (Slc26a8) is required for sperm terminal differentiation and male fertility in the mouse. Hum Mol Genet. 2007;16:1783–93.
26. Escalier D. Arrest of flagellum morphogenesis with fibrous sheath immaturity of human spermatozoa. Andrologia. 2006;38:54–60.
27. Turner TT. On the epididymis and its role in the development of the fertile ejaculate. J Androl. 1995;16:292–8.
28. Cooper TG. Cytoplasmic droplets: the good, the bad or just confusing? Hum Reprod (Oxford, England). 2005;20:9–11.
29. Gergely A, Kovanci E, Senturk L, Cosmi E, Vigue L, Huszar G. Morphometric assessment of mature and diminished-maturity human spermatozoa: sperm regions that reflect differences in maturity. Hum Reprod. 1999;14:2007–14.
30. Huszar G, Vigue L. Incomplete development of human spermatozoa is associated with increased creatine phosphokinase concentration and abnormal head morphology. Mol Reprod Dev. 1993;34:292–8.
31. Huszar G, Vigue L. Spermatogenesis-related change in the synthesis of the creatine kinase B-type and M-type isoforms in human spermatozoa. Mol Reprod Dev. 1990;25:258–62.
32. Huszar G, Vigue L, Corrales M. Sperm creatine kinase activity in fertile and infertile oligospermic men. J Androl. 1990;11:40–6.
33. Cooper TG, Yeung CH. Acquisition of volume regulatory response of sperm upon maturation in the epididymis and the role of the cytoplasmic droplet. Microsc Res Tech. 2003;61:28–38.
34. Nagata K, Asano T, Nozawa Y, Inagaki M. Biochemical and cell biological analyses of a mammalian septin complex, Sept7/9b/11. J Biol Chem. 2004;279:55895–904.
35. Cesario MM, Bartles JR. Compartmentalization, processing and redistribution of the plasma membrane protein CE9 on rodent spermatozoa. Relationship of the annulus to domain boundaries in the plasma membrane of the tail. J Cell Sci. 1994;107(Pt 2):561–70.
36. Takizawa PA, DeRisi JL, Wilhelm JE, Vale RD. Plasma membrane compartmentalization in yeast by messenger RNA transport and a septin diffusion barrier. Science. 2000;290:341–4.